Effect of Mo Addition on Structure and Magnetocaloric Effect in γ-FeNi Nanocrystals

HUSEYIN UCAR,[1,3] MARK CRAVEN,[2] D.E. LAUGHLIN,[1] and M.E. MCHENRY[1]

1.—Materials Science and Engineering, Carnegie Mellon University, Pittsburgh, PA, USA. 2.—Department of Biology, Carlow University, Pittsburgh, PA, USA. 3.—e-mail: hucar@andrew.cmu.edu

Nanocrystalline powders of $(Fe_{70}Ni_{30})_{100-x}Mo_x$ (x = 1 to 4) were produced by high-energy (SPEX) mechanical alloying. Increasing the Mo content was found to stabilize the face-centered cubic phase in mechanically alloyed nanopowders. To obtain a single γ-phase, a powdered sample was solution annealed in the γ-phase field and water quenched. The Curie temperature, T_C, of the alloys was lowered with Mo addition, without decreasing the refrigeration capacity (RC), due to the additional temperature broadening of the magnetic entropy change. Based on previous study on the role of disorder, the additional temperature broadening was attributed to increased positional disorder and changes in the distribution of ferromagnetic exchange bonds introduced by Mo addition into the γ-FeNi system. $(Fe_{70}Ni_{30})_{97}Mo_3$ and $(Fe_{70}Ni_{30})_{96}Mo_4$ alloys have RC_{FWHM} values of $\sim$440 J/kg and $\sim$432 J/kg at 5 T, comparable to other prominent magnetic refrigerants operating near room temperature. The economic viability of these alloys, along with their competitive magnetocaloric properties and potential for scalable production, make them good candidate magnetic refrigerants without critical rare-earth materials.

Key words: Nanostructured FeNi, magnetocaloric effect, magnetic refrigeration, mechanical alloying, ball milling

INTRODUCTION

The magnetocaloric effect (MCE) is defined as the temperature change of a magnetic material upon the application of a magnetic field. As the magnetic field increases entropy of the spin subsystem decreases, it is balanced by an increase in the entropy of the lattice under adiabatic conditions. This increase in the lattice subsystem promotes heating of the material.[1] The temperature rise due to losses is a limiting factor in magnetic components for high-frequency power electronics,[2] and MCE can contribute to passive cooling to control heating in high-power conversion applications. The MCE has been investigated for various materials that operate at high temperatures. However, the trend in MCE research is shifting towards synthesizing magnetocaloric materials for room-temperature applications with high efficiency and reduced cost, as well as trying to reduce or eliminate reliance on strategic rare-earth materials. To achieve this goal, transition metals have been investigated to replace rare-earth metals for cost reduction. Researchers have been able to reduce cost through use of transition metals while obtaining magnetocaloric responses comparable to those of rare-earth metals. Recently, Fe-Ni alloys were suggested as economical alternatives[3] whose RC could be tuned by alloying and the breadth of the magnetic transition controlled by impurity and disorder-derived distributed exchange interactions.[4,5]

Our earlier study showed that binary FeNi with $Fe_{70}Ni_{30}$ stoichiometry has the highest magnetic

moment in the γ-phase, with T_C slightly above room temperature.[6] The aim of this study is to show the effect of the γ-stabilizer, Mo, on the structure and magnetic properties of γ-FeNi nanocrystals. The possibility of tuning the Curie temperature (T_C) of γ-FeNi near room temperature by small additions of Mo is also discussed. Addition of Mo to the γ-FeNi system also promotes high initial permeability and increased electrical resistivity.[7]

EXPERIMENTAL PROCEDURES

Alloys of $(Fe_{70}Ni_{30})_{100-x}Mo_x$ ($x = 1$ to 4) were produced via ball milling. For simplicity, $Fe_{70}Ni_{30}$ is designated as FeNi and $(Fe_{70}Ni_{30})_{100-x}Mo_x$ alloys from $x = 1$ to 4 are designated as Mo_1, Mo_2, Mo_3, and Mo_4, respectively. Elemental Fe (125-mesh particle size), Ni (100-mesh particle size), and Mo (100-mesh particle size) were mixed and sealed in a steel vial in Ar atmosphere. Ball milling was performed with a SPEX 8000 mixer/mill using hardened-steel vials and balls with ball-to-powder weight ratio of 10:1 for 30 h. Previous studies indicated that 12 h is sufficient time to reach a steady-state microstructure.[8]

After 30 h of milling, powders were characterized using a Philips X'Pert multipurpose diffractometer (MPD) working in continuous scanning mode with Cu K_α radiation ($\lambda = 0.154056$ nm). Magnetic properties were studied using a Lakeshore 7407 vibrating-sample magnetometer (VSM) using a maximum applied field of 0.55 T. For low-temperature magnetic properties, a physical properties measurement system (PPMS) with a VSM head was used instead with a maximum applied field of 5 T. The magnetic entropy change due to the application of a magnetic field was calculated using a numerical approximation to the equation

$$\Delta S_M = \int\limits_0^{H_{max}} \left(\frac{\partial M}{\partial T}\right)_H dH, \qquad (1)$$

where ΔS_M is the magnetic entropy change, M is the magnetization, and T is the temperature. The partial derivative is replaced by finite differences, and the integration is performed numerically from zero to the maximum value of the applied magnetic field.

RESULTS AND DISCUSSION

X-Ray Diffraction

Structural analysis of mechanically alloyed $(Fe_{70}Ni_{30})_{100-x}Mo_x$ powders was performed by x-ray diffraction (XRD). Figure 1 shows the XRD patterns, exhibiting both body-centered cubic (bcc) and face-centered cubic (fcc) phases for all Mo concentrations. However, the fcc-to-bcc volume fraction ratio was found to increase with increasing Mo content.

The fractions of fcc and bcc phases were determined by comparing the intensities of the bcc(211) and fcc(220) peaks. Unlike the bcc(110) and fcc(111) peaks, the selected peaks do not overlap with each other, which would otherwise lead to more difficult interpretation of results. To correctly estimate the fractions of each phase, XRD peaks need to be corrected for Lorentz polarization, multiplicity, and structure factors.[9] The equation for calculating the phase fraction of each phase is[8]
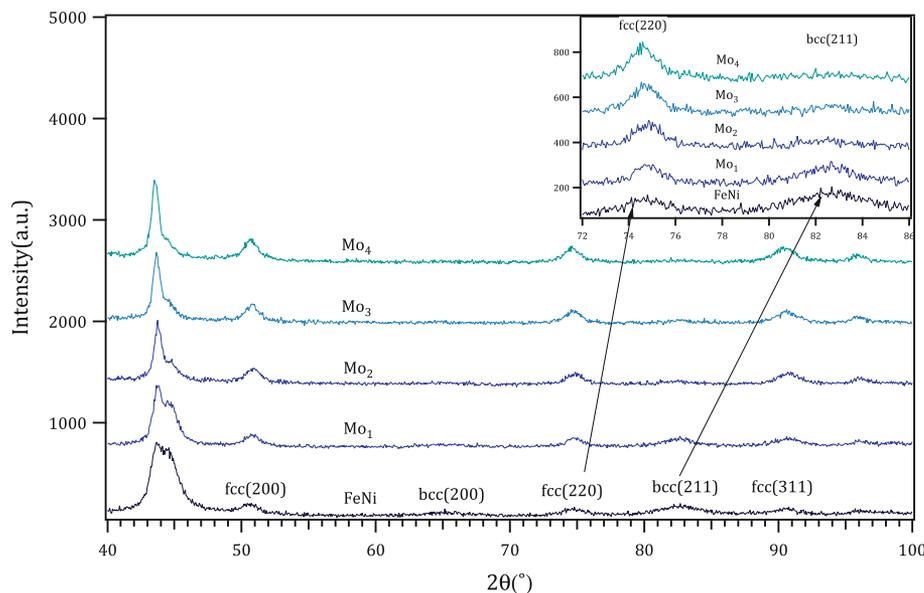

Fig. 1. x-Ray diffraction patterns of as-milled $(Fe_{70}Ni_{30})_{100-x}Mo_x$ ($x = 0$ to 4) alloys, labeled FeNi, Mo_1, Mo_2, Mo_3, and Mo_4, respectively. Inset: fcc(220) and bcc(221) peaks of as-milled $(Fe_{70}Ni_{30})_{100-x}Mo_x$ ($x = 0$ to 4) alloys.

$$\frac{f_{\text{bcc}}}{f_{\text{fcc}}} = \text{CF}\frac{I_{\text{bcc}}}{I_{\text{fcc}}}, \tag{2}$$

where f_{bcc} and f_{fcc} are the fractions of the phases, and I_{bcc} and I_{fcc} are the intensities measured from the experimental data. CF, the correction factor, can be calculated by dividing the theoretical intensity $I_{\text{theoretical(bcc)}}$ by $I_{\text{theoretical(fcc)}}$, thus

$$\text{CF} = \frac{I_{\text{theoretical(bcc)}}}{I_{\text{theoretical(fcc)}}}. \tag{3}$$

The theoretical intensity can be expressed as

$$I_{\text{theoretical}} = |F|p\left(\frac{1 + \cos^2(2\theta)}{\sin^2(2\theta)\cos(\theta)}\right), \tag{4}$$

where F is the structure factor, p is the multiplicity, and the term in parenthesis is the Lorentz polarization factor. For the bcc(211) and fcc(220) planes, the CF was calculated to be 2.62. Following this procedure, the phase fractions were calculated and are plotted versus Mo concentration in Fig. 2.

Magnetocaloric Properties

The magnetocaloric response was calculated according to Eq. 1 using isothermal magnetization curves. The magnetic entropy changes, ΔS_{M}, for the FeNi, Mo_1, Mo_2, Mo_3, and Mo_4 alloys are illustrated in Fig. 3 for a maximum applied field of 0.55 T, or 5 T for the Mo_4 alloy.

From Fig. 3a, it is obvious that small additions of Mo into $\text{Fe}_{70}\text{Ni}_{30}$ decrease the T_{C} of the alloy and the magnetic moment, which agrees well with previous studies.[10] There are two reasons for the reduction in magnetic moment with Mo addition. With addition of Mo, T_{C} reaches near room temperature, which brings about reduction in the magnetic moment. Secondly, Mo decreases the spin-up electron density of the d-band state, $n_{\text{d}}^{\uparrow}$, in the FeNi system, which reduces the magnetic moment,
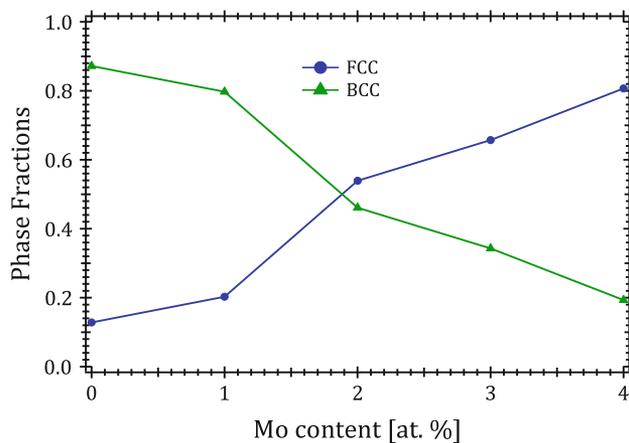
as described by the virtual bound state model.[11,12] Virtual bound state and magnetic valence models[13] have been used ubiquitously in interpreting the moment reduction in crystalline and amorphous alloys[14] due to early transition-metal addition. Even though the T_{C} of the alloys systematically decreases with Mo addition, the trend does not seem to be followed for the FeNi and Mo_1 alloys; i.e., the T_{C} of Mo_1 is slightly higher than that of FeNi. While the Mo alloys were synthesized consecutively in this study, the FeNi alloy was synthesized in a different batch, results of which were presented in our earlier study.[6] Standardizing the parameters such as the temperature, the atmosphere, and most importantly the degree of contamination during milling is not a trivial task, which might account for the slight shift of magnetic properties for the alloys produced by mechanical alloying.

Since Mo_4 has the T_{C} closest to room temperature, the magnetocaloric response of this alloy was also measured from 150 K to 480 K at field of 5 T using the PPMS (Fig. 3b). The magnetocaloric response of materials is compared using a parameter called the refrigeration capacity (RC). One well-known definition of the RC is the product of the peak entropy change times the full-width at half-maximum (FWHM) of the peak ΔT, i.e., $\text{RC}_{\text{FWHM}} = \left|\Delta S_{\text{M}}^{\text{pk}}\right|\Delta T$. According to this definition, the experimental RC_{FWHM} of Mo_4 is calculated to be 432 J/kg. For materials that did not cover sufficient area around the peak, e.g., Mo_2 and Mo_3, RC_{FWHM} was estimated by extrapolating the experimental data to the temperatures required for this calculation (Fig. 3). Moreover, for the alloys lacking experimental data at high fields, e.g., Mo_1, Mo_2, and Mo_3, the RC_{FWHM} can be expressed as a power law,[15]

$$\text{RC}_{\text{FWHM}} = AH^n, \tag{5}$$

where A is a prefactor. By extrapolating the experimental data to higher fields, one can compare the response of the alloy of interest to some benchmark refrigerants. The extrapolated and experimental values (in bold) of the alloys in this study are presented in Table I with their peak temperatures.

It can be concluded from Table I that Mo can be used as a means to tune T_{C} without compromising RC_{FWHM}. Even though the magnetic moment is slightly suppressed with addition of Mo into FeNi, the RC_{FWHM} of the Mo alloys remains virtually the same. This is attributed to the fact that the magnetic entropy curve broadens with Mo addition, which balances out the reduction resulting from the magnetic moment suppression. For maximum thermodynamic efficiency, a thermodynamic cycle is typically operated for a range of temperatures, so a large peak entropy is not necessarily desirable. This technique offers advantages over previously published routes designed to produce nanocrystal/amorphous nanocomposites[18–20] with near-room-temperature T_{C} values in terms of the size of the RC
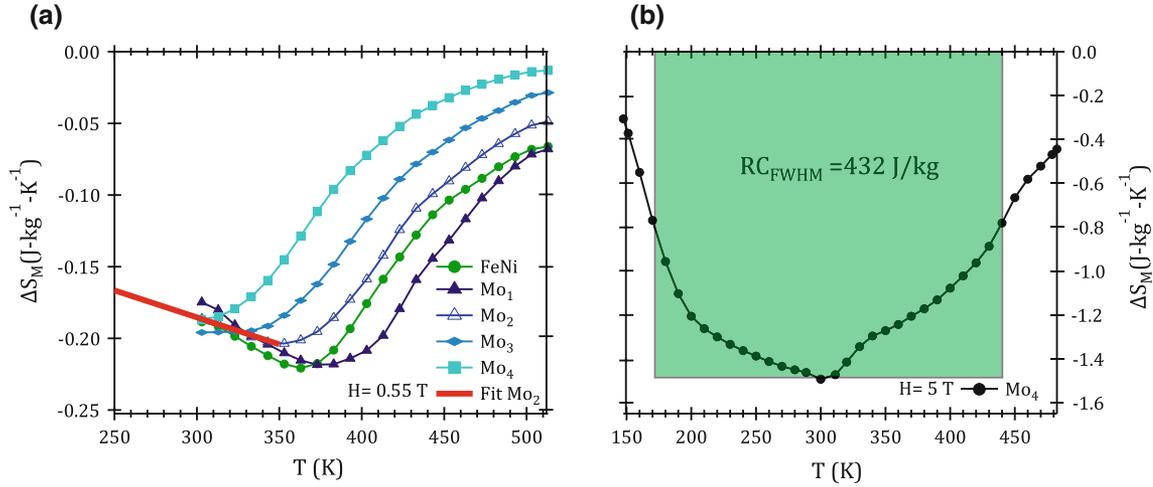

Fig. 2. Fractions of bcc and fcc phases in as-milled $(\text{Fe}_{70}\text{Ni}_{30})_{100-x}\text{Mo}_x$ (x = 0 to 4) alloys, determined by x-ray diffractometry.

Fig. 3. Temperature dependence of the magnetic entropy change, ΔS_M, of (a) solution-annealed $(Fe_{70}Ni_{30})_{100-x}Mo_x$ (x = 0 to 4) at 0.55 T (data for FeNi adapted from Ref. 6) and (b) solution-annealed $(Fe_{70}Ni_{30})_{96}Mo_4$ at 5 T.

Table I. Peak temperature (T_{pk}), peak magnetic entropy change ($\left|\Delta S_M^{pk}\right|$), and RC_{FWHM} values of promising magnetocaloric refrigerants operating near room temperature

Nominal Composition	T_{pk} (K)	$\left|\Delta S_M^{pk}\right|$ (5 T) (J kg^{-1})	RC_{FWHM} (5 T)	$\left|\Delta S_M^{pk}\right|$ (0.5 T) (Exp)	RC_{FWHM} (0.5 T) (Exp)	Ref.
$Gd_5Ge_{1.9}Si_2Fe_{0.1}$	300	7.1	**630**	–	–	16
$Fe_{88}Zr_7B_4Cu_1$	300	3.31	654	–	–	17
$(Fe_{70}Ni_{30})_{99}Mo_1$	373	1.74	460	**0.21**	**56**	This study
$(Fe_{70}Ni_{30})_{98}Mo_2$	353	1.70	445	**0.19**	**53**	This study
$(Fe_{70}Ni_{30})_{97}Mo_3$	320	1.69	440	**0.19**	**52**	This study
$(Fe_{70}Ni_{30})_{96}Mo_4$	300	1.67	**432**	**0.18**	**50**	This study

Experimental values in bold.

and cost of the alloy. It also has advantages over chemical synthesis techniques[21] in terms of the potential scalability of the process. Besides magnetocaloric applications, it may also offer possibilities for self-regulated radiofrequency (RF) heating for hyperthermia applications.[22,23]

CONCLUSIONS

Ball milling of Fe, Ni, and Mo particles for 30 h led to alloy formation as indicated by structural data. Increasing the Mo content was found to promote fcc γ-phase formation over the bcc α-phase. Mo was used to tune the T_C of the FeNi alloy without changing the RC_{FWHM} value significantly. The Mo_3 and Mo_4 alloys had peak temperatures of 320 K and 300 K, respectively, making these alloys appropriate for applications operating near room temperature such as magnetic refrigeration and self-regulated hyperthermia for cancer treatments. Even though the RC_{FWHM} values of the Mo alloys are slightly lower than those of other important refrigerants (Table I), their attractive economic viability would make them preferable alternatives for large-scale production.

REFERENCES

1. V. Franco, J.M. Borrego, C.F. Conde, and A. Conde, *J. Appl. Phys.* 100, 083903 (2006).
2. A.M. Leary, P.R. Ohodnicki, and M.E. McHenry, *JOM* 64, 772 (2012).
3. H. Ucar, J.J. Ipus, V. Franco, M.E. McHenry, and D.E. Laughlin, *JOM* 64, 782 (2012).
4. N.J. Jones, H. Ucar, J.J. Ipus, M.E. McHenry, and D.E. Laughlin, *J. Appl. Phys.* 111, 07A334 (2012).
5. K.A. Gallagher, M.A. Willard, V. Zabenkin, D.E. Laughlin, and M.E. McHenry, *J. Appl. Phys.* 85, 5130 (1999).
6. H. Ucar, J.J. Ipus, D.E. Laughlin, and M.E. McHenry, *J. Appl. Phys.* 113, 17A918 (2013).
7. R.M. Bozorth, *Ferromagnetism* (New York: D. Van Nostrand, 1951).
8. L.B. Hong and B. Fultz, *J. Appl. Phys.* 79, 3946 (1996).
9. B.D. Cullity and S.R. Stock, *Elements of X-ray Diffraction* (Menlo Park, CA: Addison-Wesley, 1996).
10. V. Franco, C.F. Conde, and A. Conde, *Appl. Phys. Lett.* 90, 052509 (2007).

11. R.C. O'Handley, *Modern Magnetic Materials, Principles and Applications* (New York, NY: Wiley, 1999).
12. J. Friedel, *Nuovo Cimento* 10, 287 (1958).
13. A. Malozemoff, A. Williams, and V. Moruzzi, *Phys. Rev. B* 29, 1620 (1984).
14. A. Ghemawat, M. McHenry, and R. O'Handley, *J. Appl. Phys.* 63, 3388 (1988).
15. V. Franco, J.S. Blázquez, and A. Conde, *Appl. Phys. Lett.* 89, 222512 (2006).
16. V. Provenzano, A.J. Shapiro, and R.D. Shull, *Nature* 429, 853 (2004).
17. R. Caballero-Flores, V. Franco, A. Conde, K.E. Knipling, and M.A. Willard, *Appl. Phys. Lett.* 96, 182506 (2010).
18. M.E. McHenry, M.A. Willard, and D.E. Laughlin, *Prog. Mater. Sci.* 44, 291 (1999).
19. J.J. Ipus, P. Herre, P.R. Ohodnicki, and M.E. McHenry, *J. Appl. Phys.* 111, 07A323 (2012).
20. J.J. Ipus, H. Ucar, and M.E. McHenry, *IEEE Trans. Magn.* 47, 2494 (2011).
21. K.L. McNerny, Y. Kim, D.E. Laughlin, and M.E. McHenry, *J. Appl. Phys.* 107, 09A312 (2010).
22. C.L. Ondeck, A.H. Habib, P.R. Ohodnicki, K. Miller, C.A. Sawyer, P. Chaudhary, and M.E. McHenry, *J. Appl. Phys.* 105, 07B324 (2009).
23. K.J. Miller, M. Sofman, K.L. McNerny, and M.E. McHenry, *J. Appl. Phys.* 107, 09305 (2010).